How to Make Tubular Crystals by Reconstitution of Detergent-Solubilized Ca²⁺-ATPase

Howard S. Young,* Jean-Louis Rigaud,# Jean-Jacques Lacapère,# Laxma G. Reddy,§ and David L. Stokes*

*Skirball Institute of Biomolecular Medicine, New York University Medical Center, New York, New York 10016 USA; #Institut Curie, Section de recherche, UMR-CNRS 168 and LCR-CEA 8, 75231 Paris, France; and §Department of Biochemistry, University of Minnesota, Minneapolis, Minnesota 55455 USA

ABSTRACT   In an attempt to better define the parameters governing reconstitution and two-dimensional crystallization of membrane proteins, we have studied Ca²⁺-ATPase from rabbit sarcoplasmic reticulum. This ion pump forms vanadate-induced crystals in its native membrane and has previously been reconstituted at high lipid-to-protein ratios for functional studies. We have characterized the reconstitution of purified Ca²⁺-ATPase at low lipid-to-protein ratios and discovered procedures that produce long, tubular crystals suitable for helical reconstruction. $C_{12}E_8$ (n-dodecyl-octaethylene-glycol monoether) was used to fully solubilize various mixtures of lipid and purified Ca²⁺-ATPase, and BioBeads were then used to remove the $C_{12}E_8$. Slow removal resulted in two populations of vesicles, and the proteoliposome population was separated from the liposome population on a sucrose density gradient. These proteoliposomes had a lipid-to-protein ratio of 1:2, and virtually 100% of molecules faced the outside of vesicles, as determined by fluorescein isothiocyanate labeling. Cycles of freeze-thaw caused considerable aggregation of these proteoliposomes, and, if phosphatidyl ethanolamine and phosphatidic acid were included, or if the bilayers were doped with small amounts of $C_{12}E_8$, vanadate-induced tubular crystals grew from the aggregates. Thus our procedure comprised two steps—reconstitution followed by crystallization—allowing us to consider mechanisms of bilayer formation separately from those of crystallization and tube formation.

INTRODUCTION

A great deal of cellular physiology occurs at the membrane, and membrane proteins therefore play a central role in a wide range of activities, e.g., signaling, transport, and motility. A wide range of methodologies have been used to identify and study the function of these membrane proteins, but structural studies remain relatively rare. Nevertheless structural studies are often critical to developing an understanding of structure-function relationships, as illustrated by the handful of membrane protein structures determined so far at atomic resolution, either by x-ray crystallography (Deisenhofer et al., 1985; Iwata et al., 1995; Picot et al., 1994; Weiss et al., 1990) or by electron microscopy (Henderson et al., 1990; Kühlbrandt and Wang, 1991). Furthermore, many lower resolution structures, determined exclusively by electron microscopy, have also been helpful in determining, for example, the basic molecular shape, the distribution of mass relative to the membrane, the physical location of specific sites on the molecule, or the structure of different molecular conformations.

Unlike the three-dimensional crystals of detergent-solubilized proteins used for x-ray crystallography, electron microscopy has for the most part been done with two-dimensional crystals within a membrane. These crystals sometimes form in specialized cellular membranes in which a particular membrane protein is highly concentrated (e.g., electric organ, Brisson and Unwin, 1984; and sarcoplasmic reticulum, Dux and Martonosi, 1983) or even naturally ordered (e.g., purple membrane, Blaurock and Stoeckenius, 1971; and gap junctions, Revel and Karnovsky, 1967). In the majority of cases, however, membrane proteins have been purified (usually from natural sources) and reconstituted into artificial membranes, where they form crystals. The latter approach will become increasingly important in future studies because the vast majority of membrane proteins occur at very low levels in their native membranes, and structural studies will therefore rely on protein that has been overexpressed in cell culture. If one has been successful in obtaining sufficient quantities of expressed protein, one should of course attempt to grow three-dimensional crystals in detergent, which would potentially lead to an atomic structure by x-ray crystallography. However, success in such an endeavor is relatively rare, probably because of the difficulty in simultaneously accommodating both intramembranous and extramembranous domains within the crystal lattice (Garavito et al., 1996; Kühlbrandt, 1988). Reconstitution and two-dimensional crystallization within lipid bilayers (Jap et al., 1992; Kühlbrandt, 1992) requires less material and may be technically easier because the bilayer represents the protein's native environment. If successful, routine electron microscopy could be used for structure determination at intermediate resolution and, in favorable cases, a high-resolution structure or even an atomic model might be obtainable, given well-ordered crystals and modern methods of cryoelectron crystallography. To develop a systematic approach to two-dimensional crystallization, we have explored in this report the parameters for successful

reconstitution and crystallization of Ca^{2+}-ATPase from sarcoplasmic reticulum (SR).

Ca^{2+}-ATPase is an ATP-driven calcium pump that belongs to the family of P-type ion pumps (Pederson and Carafoli, 1987). When isolated from fast-twitch skeletal muscle, two-dimensional crystals can be formed within the native membrane. In fact, two different types of crystals have been observed, depending on incubation conditions (Dux and Martonosi, 1983; Dux et al., 1985), and one of these has been used for three-dimensional reconstruction by cryoelectron microscopy (Taylor et al., 1986b; Toyoshima et al., 1993a). These latter crystals were grown in the absence of calcium and in the presence of vanadate, which inhibits all P-type ion pumps (Pederson and Carafoli, 1987). Indeed, two other members of this family, Na^+/K^+-ATPase (Skriver et al., 1981) and H^+/K^+-ATPase (Rabon et al., 1986), have also been crystallized in the presence of vanadate, although the resulting crystals were much smaller and less ordered than those of Ca^{2+}-ATPase. Interestingly, the very long tubular crystals of Ca^{2+}-ATPase used for our three-dimensional reconstruction are not generally obtained from standard preparations of SR (Champeil et al., 1978; Eletr and Inesi, 1972; MacLennan, 1970; Meissner et al., 1973), which produce mostly small crystalline patches on spherical vesicles with an occasional short tube (Fig. 1; also see Taylor et al., 1986a,b). We wanted, therefore, to investigate the physical-chemical parameters that produce long helical tubes of Ca^{2+}-ATPase as well as to characterize its reconstitution at the low lipid-to-protein ratios required for crystallization.

Of course, there has been a long history of reconstitution of membrane proteins in general and Ca^{2+}-ATPase in particular (reviewed by Rigaud et al., 1995). Four basic strategies have evolved, based on 1) the use of organic solvents, 2) freeze-thaw and sonication, 3) protein incorporation into preformed vesicles doped with low amounts of detergents, and 4) detergent removal from fully solubilized protein and lipid. In the case of Ca^{2+}-ATPase, Rigaud and colleagues (Levy et al., 1992) have shown the last method to be most successful. However, the object of their work was to study protein function (Levy et al., 1990c; Yu et al., 1993), and the parameters of the reconstitutions were therefore optimized for the relevant functional assays. Thus their very successful protocols generated a population of proteoliposomes that were homogeneous in terms of size and lipid-to-protein ratio. For crystallization, however, the lipid-to-protein ratio should be as low as possible (e.g., 1:2 by weight, as in native SR, rather than the ratio of 40–80:1 used for functional assays), and the homogeneity is not important, as nicely formed tubes can ultimately be selected for imaging from a larger population of vesicles. In addition to such functional reconstitutions, two-dimensional crystals have been grown from a wide range of membrane proteins by removing detergent from a fully solubilized mixture of protein and lipid. These crystallization studies have not generally characterized the function of the protein, but have been designed as crystallization trials in which the size and order of any resulting crystals represent the main criterion for success; the mechanisms of reconstitution have therefore mostly been considered in retrospect (Dolder et al., 1996; Engel et al., 1992; Jap et al., 1992; Kühlbrandt, 1992). Because reconstitution of Ca^{2+}-ATPase is a step distinct from crystallization, we have attempted to consider the process from both points of view: the parameters governing protein incorporation into a forming bilayer as well as those affecting the size and morphology of the resulting crystals.
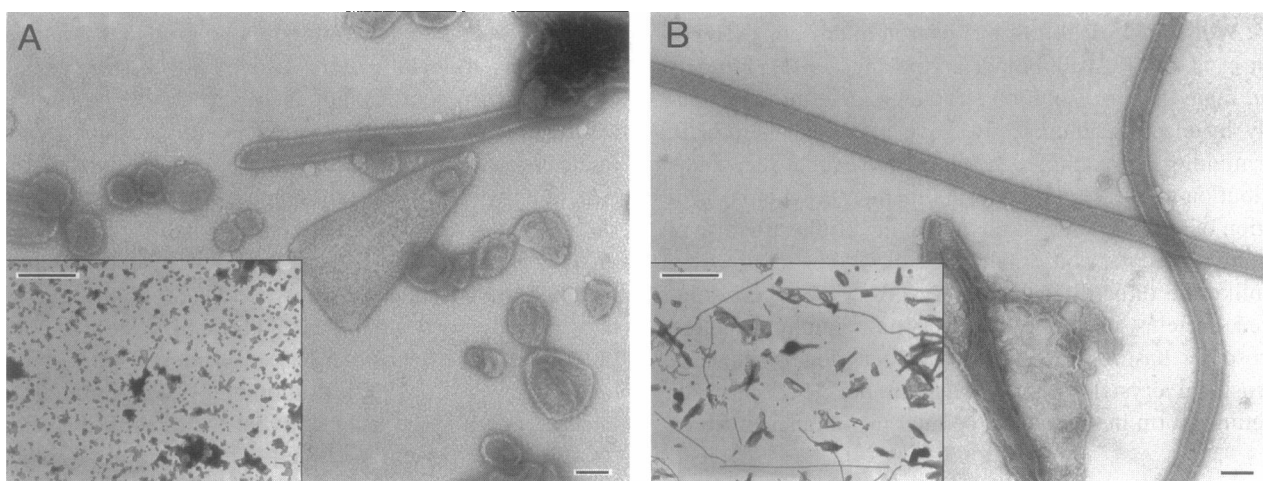

FIGURE 1 Crystal morphology in two different negatively stained SR preparations. (A) A standard preparation of SR produces crystalline vesicles and occasional short, tubular crystals. The low-magnification image (inset) shows that most of the preparation consists of small vesicles with only one short tube seen in the center of the image, which is also shown at higher magnification. The triangular vesicle nearby has crystalline arrays at its edges and seems to be devoid of protein in the middle; this eccentric shape is common and is likely a result of the high membrane curvature induced by crystallization of Ca^{2+}-ATPase. (B) An unusual SR preparation that fortuitously produces many very long tubes. Short tubes often appear to be wrapped up inside large vesicles and to break free as crystallization proceeds over a period of several days. The goal of the current work is to elucidate physical-chemical parameters that favor tubes over crystalline vesicles. Scale bars represent 0.1 μm and 2.7 μm (inset).

In particular, we have started with reconstitution methods elaborated by Rigaud and colleagues (Levy et al., 1992) and have attempted to determine which factors lead eventually to long, tubular crystals of reconstituted Ca^{2+}-ATPase that are suitable for frozen-hydrated electron microscopy and helical image analysis.

MATERIALS AND METHODS

Preparation of SR and purification of Ca^{2+}-ATPase

Skeletal SR vesicles were prepared from the white muscle in the hind legs of rabbit by the method of Eletr and Inesi (1972). Ca^{2+}-ATPase was purified from SR vesicles by affinity chromatography using Reactive Red 120 (Sigma Chemical Corp.) as described previously (Stokes and Green, 1990). After eluting the purified Ca^{2+}-ATPase from the column in 4 mM ADP, 20 mM 3-(N-morpholino)propane-sulfonic acid (pH 7.0), 1 mM $MgCl_2$, 1 mM $CaCl_2$, 20% glycerol, and 0.1% $C_{12}E_8$ (n-dodecyl-octaeth-ylene-glycol monoether), the peak fractions were pooled to give a protein concentration of 3–4 mg/ml. Purified Ca^{2+}-ATPase was determined to be >98% pure by sodium dodecyl sulfate-polyacrylamide gel electrophoresis and Coomassie blue staining; the specific ATPase activity was ~10 μmol/mg/min at 25°C when assayed in the detergent-solubilized state. The protein was stored at −80°C after 0.5 or 1 mg egg yolk phosphatidylcho-line (PC)/mg protein was added and was found to retain full activity for at least 6 months.

Reconstitution

Typically, reconstitution was carried out in a 0.5-ml solution containing 1 mg/ml Ca^{2+}-ATPase, 1 mg/ml lipid (various mixtures of PC, egg yolk phosphatidylethanolamine (PE), brain phosphatidylserine (PS), egg yolk phosphatidic acid (PA), and cholesterol, all from Avanti Polar Lipids), 2 mg/ml detergent (either $C_{12}E_8$, Nikko Chemical Corp., or Triton X-100, Sigma Chemical Corp.), 20 mM imidazole (pH 7), 100 mM KCl, and 3 mM NaN_3. The detergent was removed by adding BioBeads SM2 (BioRad Corp.) and by stirring at room temperature (Levy et al., 1990a,b). Before use, BioBeads were washed several times in methanol followed by several more washes in distilled water and stored in water at 4°C; for use in reconstitution, excess water was aspirated away from the BioBeads, and a small quantity was quickly weighed to prevent drying. The rate of deter-gent removal was controlled by the regimen of BioBead addition. For "slow" detergent removal, 1 mg of hydrated BioBeads was added, followed by 30 min of incubation; this was repeated three more times (total of 4 mg BioBeads and 2 h of incubation), and then 6 mg of BioBeads was added and incubated for 1 h. Finally, 10 or more milligrams of BioBeads was added and incubated for an additional hour to ensure full removal of detergent (total of 20 mg BioBeads/mg $C_{12}E_8$). For "fast" detergent re-moval, the entire 20 mg of BioBeads was added at once, and the solution was then incubated for 4 h without further additions. For Triton X-100, we followed the same regimens, except that twice as much BioBeads was used (40 mg BioBeads/mg Triton X-100). Reconstituted vesicles were then separated from the BioBeads with a micropipette.

Sucrose density purification and freeze-thaw

Sucrose density gradient centrifugation was used to separate the two populations of reconstituted vesicles that resulted from slow $C_{12}E_8$ re-moval. The discontinuous sucrose gradient consisted of 400-μl layers of 10%, 20%, 30%, 40%, 50% sucrose (weight/volume) and contained 20 mM imidazole (pH 7), 100 mM KCl, and 3 mM NaN_3. After loading reconstituted vesicles (~0.5 ml) on the top of this gradient, it was centrifuged at 100,000 × g at 4°C for 3.5 h (TLS 55 rotor in Beckman TL Optima Centrifuge). Two bands were obtained, one at the interface between 40% and 50% sucrose and

the other near the top of the gradient. Generally, the lower band was collected for crystallization with a micropipette (~0.5 ml); however, for lipid and protein determination, 0.2-ml fractions were collected from the bottom of the tube with a peristaltic pump.

Before crystallization, ~0.2 ml of the sucrose gradient fraction was diluted to ~1.5 ml in a microfuge tube (the remainder of the fraction was frozen, stored, and used at a later time) and centrifuged at 32,000 × g for 20 min at 4°C (Biofuge 22R; Baxter Scientific Products). The pellet was gently resuspended with a micropipette in 20 mM imidazole (pH 7) and 100 mM KCl and centrifuged again to wash away residual sucrose. To this pellet, 25 μl of crystallization buffer (see below) was added, followed by two cycles of freeze-thaw (freezing in liquid N_2 and thawing by holding the tube between thumb and forefinger until just thawed). Thereafter the pellet was gently resuspended with a micropipette, followed by two additional cycles of freeze-thaw.

Crystallization

Crystallization simply involved incubating a given preparation in 20 mM imidazole, 100 mM KCl, 5 mM $MgCl_2$, 0.5 mM EGTA, and 0.5 mM Na_3VO_4 on ice after adjusting the pH to 7.4 at 4°C. Na_3VO_4 was specially prepared to maximize the decameric species of vanadate as follows: a 50 mM stock solution of Na_3VO_4 was acidified to pH 2, cooled on ice, and then adjusted to pH 6.5 before addition to ice-cold crystallization buffer. The strong yellow color indicated the existence of decavanadate, and accordingly, decavanadate was visible in crystallization solutions, even after a week of incubation on ice. In many cases, 28 μM thapsigargin (LC Services Corp., Woburn, MA) was added from a 1 mM stock solution in ethanol, and in other cases 28 μM cyclopiazonic acid (Sigma Chemical Co.) was added from a 5 mM stock solution in dimethyformamide. Con-centrated SR stock was simply diluted into crystallization solution, whereas sucrose gradient fractions were resuspended in the solution before freeze-thaw. For studies of lipid-to-protein ratio, crystallization was induced before sucrose gradient purification by microdialysis in 50-μl buttons (Cambridge Repetition Engineers, Cambridge, England). In all cases, the protein concentration during crystallization was 1–2 mg/ml. Although crystallization within vesicles occurred after 1 day, 4–7 days were required for tubes to be maximally present.

Electron microscopy

Vesicles were negatively stained by pipetting 3–5 μl onto glow-discharged, carbon-coated grids and then by rapidly rinsing with three to five drops of ice-cold uranyl acetate (2%). Frozen-hydrated samples were prepared on perforated carbon films that had been glow discharged in amyl amine vapor; ~5 μl of crystal suspension was placed on a grid, and after blotting, these grids were plunged into an ethane slush. Images were recorded on a Philips (Mahwah, NJ) CM12 electron microscope at various magnifica-tions, and a Gatan (Pleasanton, CA) 626 cryoholder was used to keep frozen-hydrated samples at −170°C during imaging. For helical recon-struction, images were recorded at a magnification of 45,000× and digi-tized at 13-μm intervals with a PDS1010GM microdensitometer (Orbital Sciences Corp, Pomona, CA). Image processing was performed with a suite of programs developed by Dr. C. Toyoshima (University of Tokyo) for helical reconstruction of tubular crystals (Toyoshima and Unwin, 1990). The reconstruction presented is from two images of a single tube taken at 1 μm and 2 μm under focus. The equators were corrected for the contrast transfer function (CTF), assuming 6% amplitude contrast (Toyoshima et al., 1993b); the remaining data were averaged together to yield a reasonably flat CTF, as described by Toyoshima and Unwin (1988). Data were only used within the first zero of the CTF, thus limiting the resolution to ~20 Å.

Other assays

ATPase activity was measured at 25°C by a coupled enzyme assay (Warren et al., 1974) containing 100 mM KCl, 50 mM imidazole (pH 7), 5 mM
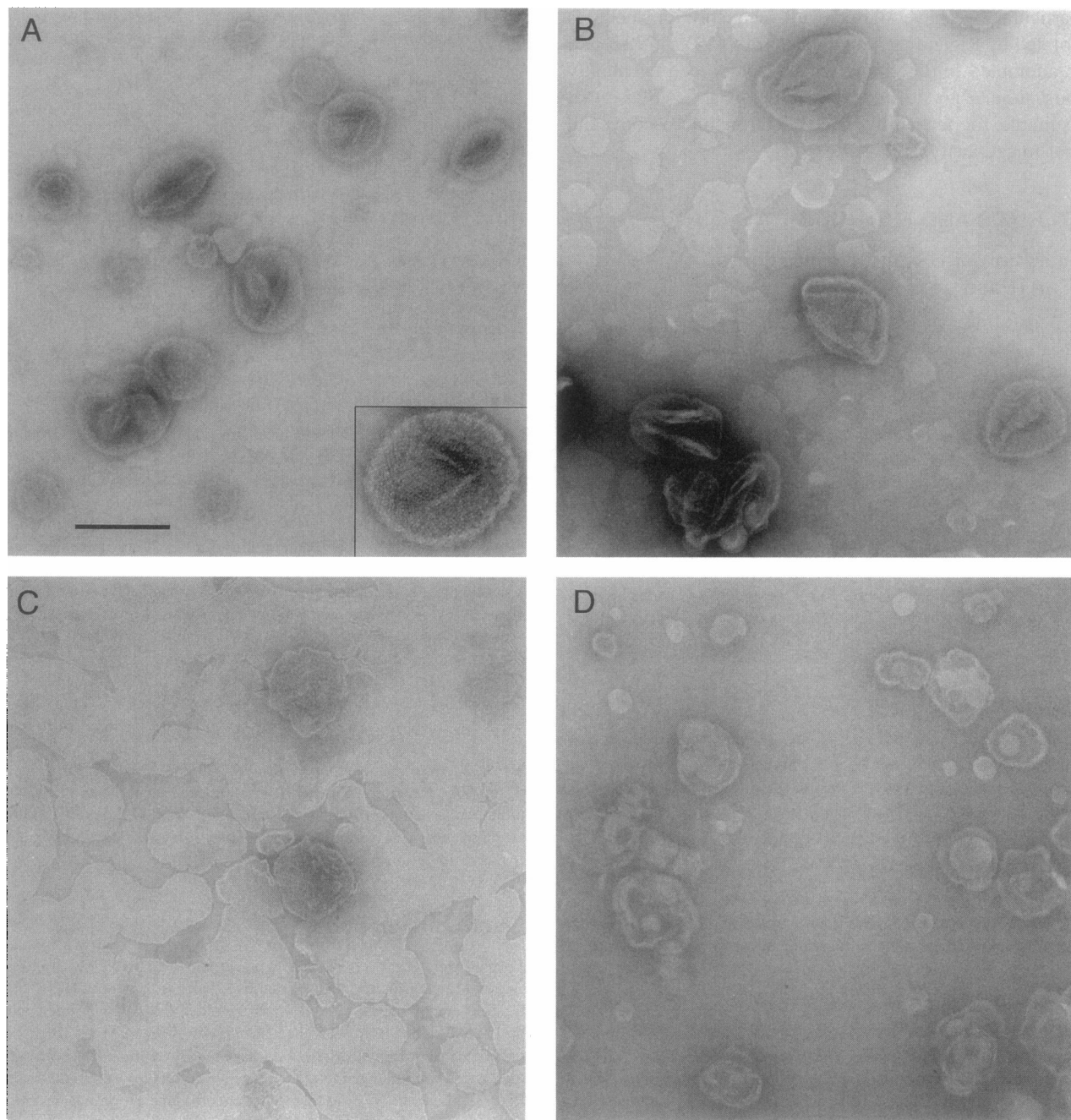
FIGURE 2   Effect of lipid-to-protein ratio on reconstitution. Reconstituted vesicles were negatively stained after incubation in crystallization solution. (A–C) Series of reconstitutions by slow removal of $C_{12}E_8$ with increasing lipid-to-protein ratios: 1:2 (A), 1:1 (B), and 4:1 (C). The darkly stained vesicles have a high protein density, and two-dimensional arrays are often visible (*inset* in A), whereas the lightly stained vesicles in B and C are pure liposomes (see Fig. 3). (D) Vesicles reconstituted by rapid removal of Triton X-100 at a 4:1 lipid-to-protein ratio. In this case, only one population of vesicles is present, and they appear to be more lipid-rich than the darkly stained vesicles obtained from $C_{12}E_8$; in this case, no crystalline arrays were seen, probably because the protein density in the vesicles was too low. The scale bar applies to all panels and corresponds to 200 nm.

MgCl$_2$, 0.1 mM CaCl$_2$, 2.4 mM ATP, 0.18 mM NADH, 0.5 mM phosphoenolpyruvate, 10 units/ml lactate dehydrogenase, 10 units/ml pyruvate kinase, and either 1 μg/ml A23187 or 0.2 mg/ml $C_{12}E_8$. Protein concentrations were determined with the procedure of Lowry (Lowry et al., 1951), as modified for membrane proteins by Markwell et al. (1978). Lipid phosphorous determination was based on forming a phosphomolybdate complex, as originally described by Chen et al. (1956) and modified by Chester et al. (1987).

RESULTS

Lipid-to-protein ratio

Following the guidelines laid out by Rigaud and colleagues for reconstitution of Ca^{2+}-ATPase from a fully solubilized state (Levy et al., 1992), we studied its crystallization after
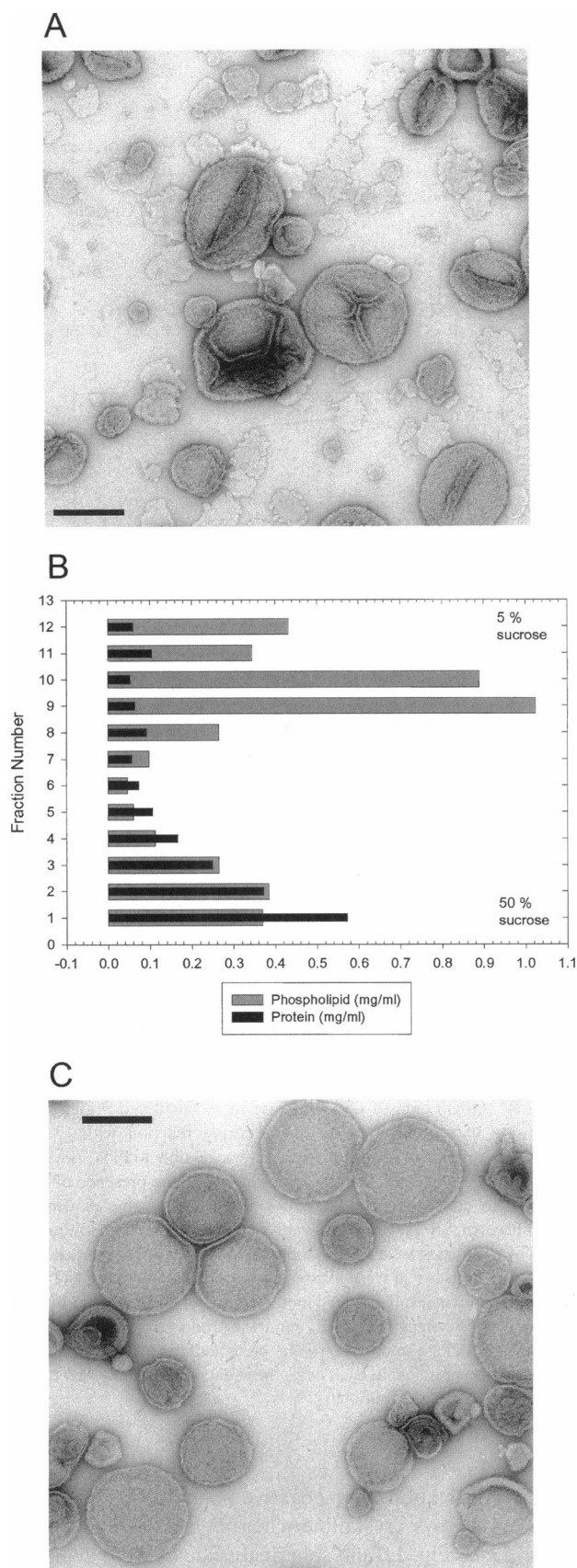
decreasing the lipid-to-protein ratios near those found in the native SR membrane. We conducted such studies many times over a period of several years in several different laboratories, and in virtually all cases we were able to induce crystallization of Ca^{2+}-ATPase in the resulting vesicles. However, the appearance of vesicles and the extent of the array formation depended primarily on the lipid-to-protein ratio, which ranged between 4:1 and 1:4 by weight. For example, when a total of 0.5–0.75 mg lipid/mg protein was included in the reconstitution, a homogeneous population of well-stained vesicles was obtained, and after incubation in vanadate-containing crystallization buffer, these vesicles showed a high degree of crystallinity (Fig. 2 A). If a larger amount of lipid was added and detergent was removed slowly (i.e., by incremental addition of BioBeads over 3–4 h), a second population of vesicles was observed, which stained poorly (Fig. 2 B) and which contained relatively little protein (see below). The proportion of vesicles in this second population increased with increasing lipid content (Fig. 2 C). Crystalline patches were usually present in the well-stained vesicles, but tended to be smaller and less abundant at the higher lipid-to-protein ratios. The appearance of vesicles was less heterogeneous if the detergent was removed more rapidly or if Triton X-100 was used instead of $C_{12}E_8$ (Fig. 2 D). These vesicles tended to be more crenulated, characteristic of a higher lipid content, and crystalline patches were rarely observed.

The two vesicle populations generated by slow detergent removal were separated by sucrose density gradient centrifugation, thus allowing us to measure their respective lipid-to-protein ratios (Fig. 3). The well-stained vesicles were relatively dense and equilibrated at ~40% sucrose; their lipid-to-protein ratio was determined to be 1:2 by measuring phosphate and protein contents in the relevant fraction. In contrast, the poorly stained vesicles were much less dense and equilibrated at ~5% sucrose; these vesicles appeared to be virtually pure lipid, because their protein content was no higher than background levels.

Sidedness of protein insertion

In addition to protein density, we investigated the orientation of Ca^{2+}-ATPase in the bilayer after reconstitution. This was done by determining the fraction of molecules accessible to fluorescein isothiocyanate (FITC), which undergoes a well-characterized reaction with Lys 515 in the cytoplas-

FIGURE 3   Sucrose density gradient purification. Reconstituted vesicles were made with a 1:1 lipid-to-protein ratio (A) and loaded on a sucrose density gradient. Fractions were collected from the gradient and assayed for protein and lipid content (B). Two bands of vesicles were visible after centrifugation: the one at the top consisted of virtually pure liposomes, whereas the bottom band had vesicles with a 1:2 lipid-to-protein ratio. Electron microscopy of vesicles from the bottom band (C) showed that, unlike the starting material (A), they were homogeneous and consisted only of the darkly staining vesicles (also see Fig. 2 A–C). The scale bars correspond to 200 nm.

mic domain, thus abolishing the ATPase activity of Ca^{2+}-ATPase (Mitchinson et al., 1982). Accordingly, we took the residual ATPase activity after full reaction with FITC to represent the fraction of Ca^{2+}-ATPase molecules facing the inside of intact, reconstituted vesicles; SR and detergent-solubilized, reconstituted vesicles represented controls in which all molecules were accessible to FITC. Fig. 4 shows that reaction with FITC was complete after 20–40 min, although the rate of inactivation depended somewhat on the nature of the preparation and on the presence of detergent. Residual activity was ~20% of unreacted controls in vesicles reconstituted by fast detergent removal and 0% in vesicles made by slow detergent removal, suggesting that the fractions of Ca^{2+}-ATPase molecules facing outward were 80% and 100%, respectively. As expected, both SR and detergent-permeabilized vesicles were fully inhibited by FITC; for SR, this indicates that all molecules were outward facing, whereas permeabilization provided FITC access to all molecules, regardless of the side of the vesicle they faced.

Vesicle fusion and tube formation

Because SR vesicles are relatively small (50–200 nm diameter) and tubes are often 5–10 μm long, we expected that fusion would be required for formation of these tubes. Thus the fusogenicity of individual preparations of SR might explain their differing capacity for forming tubes. Reconstituted proteoliposomes are of a size similar to that of SR vesicles, and we therefore investigated conditions for fusion of proteoliposomes both before and during crystallization. The first concern was to remove the lipid-rich vesicles to prevent them from fusing with protein-rich vesicles, thus reducing the protein density in the bilayer. Separation of these two populations by sucrose density gradient (Fig. 3) was therefore an important first step. Fusion was then attempted by several cycles of freeze-thaw, generally inducing a large amount of vesicle aggregation, but causing only a modest increase in the size of some vesicles. However, our ultimate criterion for success was the number of tubes present after crystallization, and it was not possible to predict this outcome simply by observing the size of vesicles produced by freeze-thaw. By much trial and error, we found that removing sucrose and maintaining a relatively high vesicle concentration (>1 mg protein/ml) were critical for obtaining a high frequency of tubes. Specifically, the most successful procedure involved pelleting vesicles after sucrose density purification and subjecting this pellet to several cycles of freeze-thaw; this tended to break up the pellet, and after resuspension in crystallization buffer, several more cycles of freeze-thaw were carried out. If lipid composition was correct, several days of incubation in crystallization buffer produced a significant proportion of tubular crystals growing out of vesicle aggregates.

The abundance of these tubular crystals relative to spherical vesicles was easily detected in the electron microscope
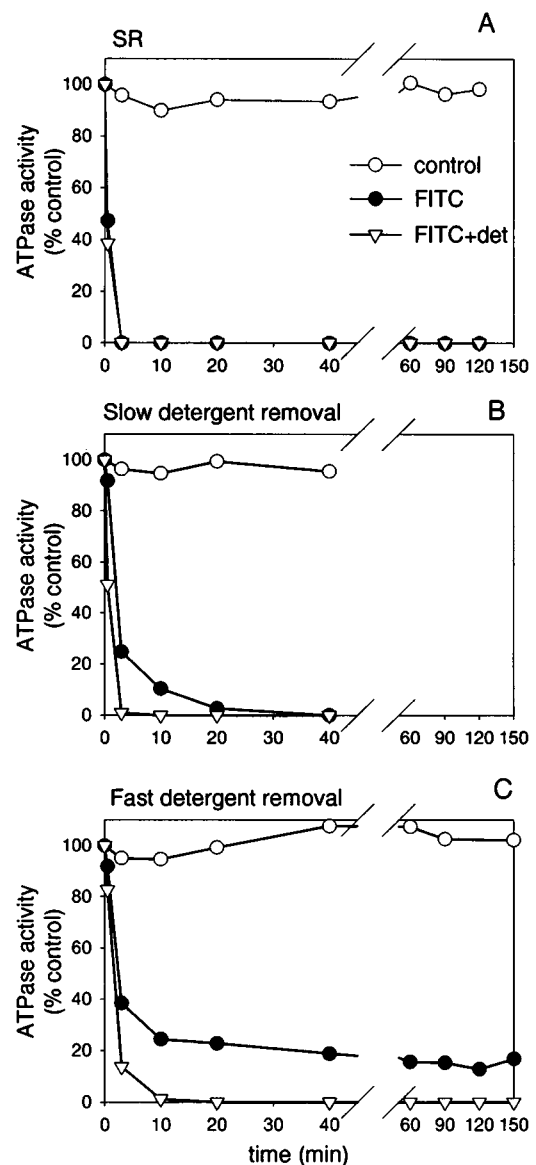

FIGURE 4 Orientation of Ca^{2+}-ATPase in reconstituted vesicles. ATPase activity of vesicles was measured during reaction with FITC to determine the fraction of molecules that were accessible to FITC (i.e., were inhibited). ATPase activity was always measured in the presence of detergent to make conditions consistent for the various samples. Because Ca^{2+}-ATPase in SR is 100% outward facing, complete inhibition was obtained by incubation with FITC in both the presence (∇) and absence ($\bullet$) of detergent; controls (O) were incubated in the absence of both FITC and detergent. A similar result was obtained for vesicles reconstituted by slow $C_{12}E_8$ removal, whereas fast $C_{12}E_8$ removal produced vesicles in which 20% of Ca^{2+}-ATPase molecules were protected from FITC, i.e., were facing inside the vesicles. In each case, these data represent the average of three independent reconstitutions.

at low magnification after negative staining (Fig. 5). Such tubes were always crystalline when viewed at higher magnification (see Fig. 1), and spherical vesicles were generally covered with ordered arrays of Ca^{2+}-ATPase molecules (see Fig. 2). Through many trials, we found several additional factors that were important in obtaining tubes instead

FIGURE 5 Effect of lipid composition and detergent additions on tube formation. When PC alone is used for reconstitution, spherical vesicles are the predominant species, with occasional short tubes. PS or PA increases the number of tubes, and the combination of PC, PS, and PE (8:1:1 ratio) predominantly produces tubes, which almost always emanate from vesicle aggregates. Alternatively, the addition of small amounts of $C_{12}E_8$ (0.16 mg/ml, corresponding to a 1:5 detergent-to-lipid ratio in this example) after reconstitution and freeze-thaw also generates tubes, regardless of the lipid composition. The detergent also produces a higher background composed of small membrane fragments (*inset*), in which Ca^{2+}-ATPase molecules are still crystalline. The scale bar represents 3 μm.
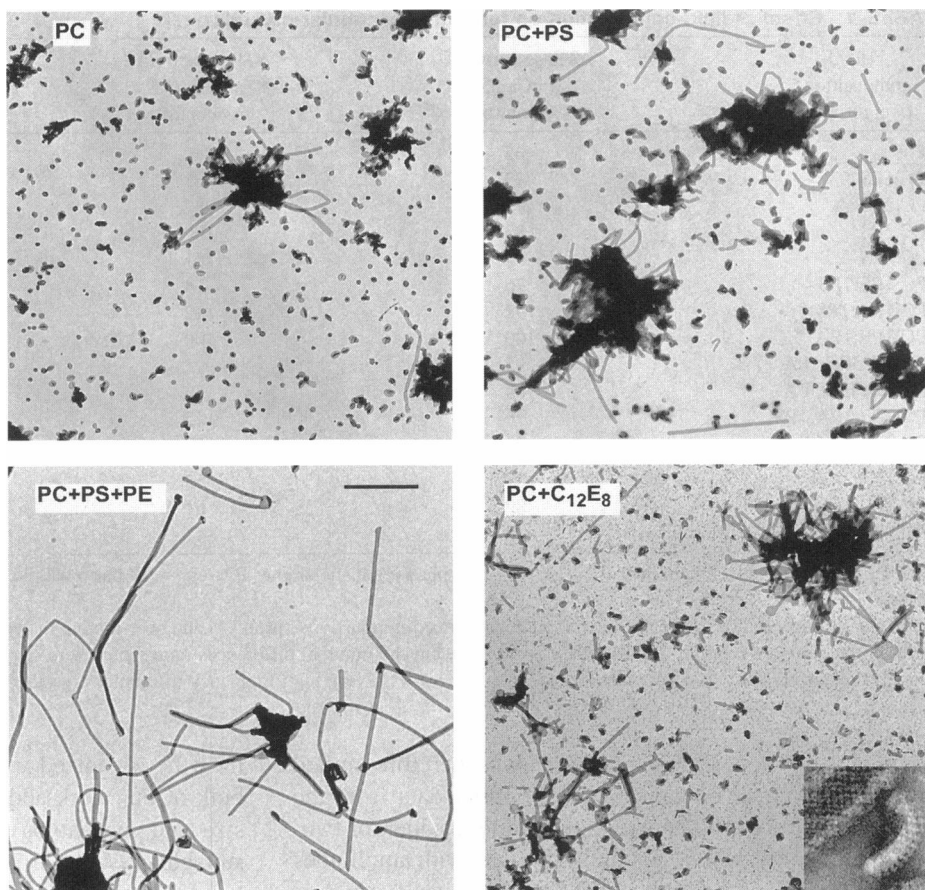
of vesicles with crystalline patches. The first was the addition of an inhibitor to lock Ca^{2+}-ATPase into a favorable conformational state. Thapsigargin was generally used for this purpose because it had previously been shown to promote and stabilize crystallization within the native SR membrane (Sagara et al., 1992). In particular, thapsigargin binds to and traps Ca^{2+}-ATPase in its calcium-free state (E_2), thus preventing further cycling. To rule out a fortuitous physical effect of the rather hydrophobic thapsigargin on the lipid bilayer, we also tested cyclopiazonic acid, which stabilizes the same conformational state (Karon et al., 1994), and found it also to be effective in tube formation. Another critical factor was the specific mixture of lipids added during reconstitution, and we tested various combinations of PC, PA, PE, PS, and cholesterol (Table 1). Although crystalline patches were observed in vesicles composed of pure PC, small amounts of PE and PA (or PS) were required for extensive tube formation. The most effective combination was 10–20% of both PE and PA (or PS), with the bulk composed of PC (Fig. 5); very high amounts of either PA or PE (50%) prevented tube formation. Crystallization was strongly suppressed by 10% cholesterol, even though activity was 50–60% of controls. Small amounts of $C_{12}E_8$ in the crystallization medium were also found to promote tube formation, even in pure PC vesicles (Fig. 5 D). The most effective concentrations of $C_{12}E_8$ were 0.05–0.2 mg/ml, which correspond to detergent-to-lipid ratios of 1–4:15, and

which are well below the amount needed to saturate the liposomes (1:2; Levy et al., 1990b). Higher $C_{12}E_8$ concentrations (>0.1 mg/ml) produced small membrane fragments, which still contained crystalline arrays of Ca^{2+}-ATPase (Fig. 5 D, *inset*).

Crystal packing in reconstituted tubes

We performed a helical reconstruction of a single frozen-hydrated tube (Fig. 6) to determine whether the crystal symmetry and molecular packing were similar to tubes grown from SR. Regardless of their source, these membranous tubes have a variable diameter, which reflects an underlying variability in the helical symmetry (Toyoshima et al., 1993a; Toyoshima and Unwin, 1990). For previous reconstructions from SR (Toyoshima et al., 1993a), we chose the narrowest tubes (~600 Å diameter), which often could be indexed with dominant 7-start and 25-start helical families (1,0;−25 and 0,1;7, according to previous nomenclature; Toyoshima and Unwin, 1990). For the current work, we used an 800-Å-diameter tube, which was indexed with 8-start and 32-start helical families; the increased diameter accommodated more molecules around the tube. Two images of the tube were recorded, and their defocus was determined to be ~1 μm and ~2 μm, respectively. Only Fourier data in the first peak of the contrast transfer

TABLE 1 Effect of lipid composition on formation of tubular crystals

Lipid composition* (weight ratio)	ATPase activity[#] at pCa 5.4 (% control)	ATPase activity[#] at pCa 6.8 (% control)	Crystalline vesicles	Tubular crystals[§]
PC	65	47	+	+
9PC:1PS	73	61	+	++
8PC:2PS	79	82	+	++
7PC:3PS	83	100	+	++
6PC:4PS	94	161	+	++
8PC:1PE:1PS	76	74	+	+++++
8PC:1PA:1PS	92	112	+	+++++
8PC:1PE:1PA	100	100	+	+++++
7.5PC:1.5PE:1PA	95	92	+	+++++
8PC:1.5PE:0.5PA	84	76	+	+++++
7PC:1PE:1PA:1PS	96	125	+	+++++
7PC:2PE:1PA	94	112	+	++
8PC:1PA:1CH	81	55	±	−
8PC:1PE:1CH	89	61	±	−
7PC:1PE:1PA:1CH	79	43	±	−

*PC, Egg yolk phosphatidylcholine; PE, egg yolk phosphatidylethanolamine; PA, egg yolk phosphatidic acid; CH, cholesterol; PS, brain phosphatidylserine.

[#]Two Ca^{2+} concentrations were used corresponding to maximum activity (pCa 5.4) and near-minimum activity (pCa 6.8); the latter should be sensitive to shifts in the apparent calcium affinity of Ca^{2+}-ATPase, but the minimal differences represented here suggest that no such shifts occurred.

[§]−, No tubular crystals; +, a few tubular crystals; +++++, a very high frequency of tubular crystals (suitable for cryoelectron microscopy).

function were used, and the resolution was therefore limited to ~20 Å. After averaging together Fourier data from the two images, the amplitude-weighted phase residual for two-fold symmetry was 11.7°, including all data with amplitudes higher than 3% of the highest off-equatorial peak, which is very similar to results previously obtained for SR tubes with p2 symmetry. This twofold symmetry was clearly visible in phases along individual layer lines (Fig. 6 C). The parameters of the unit cell taken in the middle of the membrane ($a = 62.5$ Å, $b = 114.6$ Å, and $\gamma = 73°$) were within the range previously observed for crystals in SR (Yonekura et al., 1997). Furthermore, density maps (Fig. 6, D and E) show that molecules are packed in the so-called dimer ribbons first described for crystals from SR (Castellani et al., 1985; Taylor et al., 1984), indicating that the molecular packing as well as the symmetry of our reconstituted tubes were the same as those of tubes from SR. Sections normal to the membrane show that molecules are all facing the outside of the tubes, consistent both with maps from SR tubes and with our determinations of sidedness with FITC (Fig. 4). Thus we conclude that the crystal packing induced by decavanadate in reconstituted tubes is indeed the same as that in the native SR.

DISCUSSION

Tubular or planar crystals

We have found that vanadate-induced, two-dimensional arrays are readily obtained when detergent-solubilized Ca^{2+}-ATPase is reconstituted into proteoliposomes at low lipid-to-protein ratios by BioBead-mediated detergent removal. However, for these arrays to be useful for electron crystallographic studies, a large number (thousands) of molecules must be organized into a single, coherent crystal, and the bulk of our work addressed parameters that control crystal size and morphology. Generally speaking, there are two suitable crystal morphologies: planar sheets and cylindrical tubes. Fourier reconstruction methods exist for determining the molecular structure from either morphology (Aebi et al., 1984), and each method has its advantages and disadvantages. For example, the larger size of planar sheets often allows electron diffraction to be used as an accurate source of Fourier amplitudes, but data from each crystal is confined to a two-dimensional plane through Fourier space, and a large number of tilted crystals are therefore required to obtain enough three-dimensional data for a reconstruction (Amos et al., 1982); even then, the missing cone of Fourier data makes the resolution of the map anisotropic (Henderson et al., 1990). Alternatively, a complete three-dimensional data set can be derived from a single cylindrical tube (DeRosier and Moore, 1970), but the smaller number of molecules and the continuous distribution of diffraction data along layer lines (as opposed to discrete reflections from planar crystals) combine to reduce the signal-to-noise ratio, thus limiting the resolution.

Within their native membranes, certain proteins seem predisposed toward forming tubular crystals, whereas others form planar, sheetlike crystals. It is logical to assume that the interactions between molecules induce membrane curvature in the former but not in the latter, and therefore that the association between molecules in the membrane governs the ultimate crystal morphology. Indeed, several examples of crystals from native membranes conform to this idea: both Ca^{2+}-ATPase and nicotinic acetylcholine receptor (Brisson and Unwin, 1984) have bulky domains on the outside of vesicles and small domains on the inside, and

both generate tubular crystals, whereas the more symmetrical, hydrophobic molecules like bacteriorhodopsin (Henderson and Unwin, 1975) and mitochondrial porin (Mannella, 1984) form planar crystals. However, most native membranes are not suitable for crystallization, and reconstitution of purified proteins has therefore been extensively used for crystallization. In many cases, a given protein will form both tubular and planar crystals, depending on conditions of reconstitution (Jap et al., 1992; Wang et al., 1993), and this indicates the existence of more determinants for crystal morphology than just protein shape. Although we are far from understanding all of these determinants, a few general guidelines can be drawn considering the current work in the context of previously published reports.

First we consider tubular (helical) crystals to have a relatively small radius (<500 Å), whereas larger diameter tubes are more equivalent to planar sheets. Bending of a planar structure (e.g., stable bilayer) will generate stress (Gruner, 1985), and it is the radius of curvature that determines the magnitude of this stress. Thus it will only be tubes with small radii of curvature that have bilayer properties different from those of planar sheets. Furthermore, it is virtually impossible to preserve cylindrical symmetry in the electron microscope for radii greater than 500 Å, making helical reconstruction possible only with tubes of smaller radii. Given this limitation, a review of the literature shows that molecules composing tubular crystals always have an asymmetrical orientation with respect to the membrane plane and that virtually all of these crystals have a twofold symmetry axis normal to the membrane (i.e., p2 symmetry). These two phenomena can be understood either as causes or as consequences of membrane curvature. In particular, curvature will generate different intermolecular spacings on the two sides of the membrane, thus requiring different molecular packing and an asymmetrical arrangement of molecules across the bilayer. In addition, the twofold axis may help generate membrane curvature, as illustrated in Fig. 7, where the opposite inclinations of molecules 1 and 2 relative to the twofold axis will be accommodated and perhaps stabilized by the twofold symmetry; translational symmetry and twofold axes in the plane of the membrane will tend to disfavor curvature. Furthermore, higher order symmetry (e.g., p3) will lead to bends along several different axes and therefore will lead more readily to planar or to spherical structures (e.g., icosahedral viruses). Given p2 symmetry and a tubular morphology, one expects the bulkier domains of proteins to be on the outside of tubular crystals to make longer-distance contacts at the higher radii, and this is indeed the case for Ca^{2+}-ATPase and acetylcholine receptor. However, relatively symmetrical molecules also make tubes (e.g., maltoporin, membrane domain of Band 3), and tubes of cytochrome bc_1 (Akiba et al., 1996) actually have their bulkier domains at the inner radii. This last example may be explained by the total lack of crystal contacts on the outer surface of tubes, such that the curvature is completely governed by contacts between protein domains on the inside. This can be generalized to state that the geometry of intermolecular crystal contacts will determine the curvature and that this geometry may or may not reflect the distribution of molecular mass across the bilayer.

If strict symmetry is maintained across the bilayer by the presence of a twofold (or twofold screw) axis parallel to the membrane plane, the crystals must be planar, because curvature would disrupt this symmetry. Indeed, we have found no exceptions to this in the literature, except for one study that used only optical diffraction and is therefore not very reliable (Warne et al., 1995). However, it is also possible to obtain planar crystals without this constraint, and p1, p2, p3, and p6 lattices have all been observed, suggesting that in these cases the intermolecular crystal contacts favor strict translational symmetry within the plane of the bilayer. It is possible that the limited growth of some planar crystals (e.g., Na^+/K^+-ATPase) is due to conflicting tendencies toward flatness and curvature, thus generating strain within the crystal lattice.

Mechanism of reconstitution

Previous studies of membrane protein crystallization have considered the mechanism of protein insertion into the bilayer, and everyone seems to agree that interactions between all of the components in the system—protein, detergent, and lipid—are critical to the outcome (Dolder et al., 1996; Engel et al., 1992; Jap et al., 1992; Kühlbrandt, 1992). In virtually all cases, the dominant criteria for judging this outcome were the crystal size and order, and, unlike in the current work, reconstitution and crystallization were not treated as independent steps. Nevertheless, Kühlbrandt (1992) pointed out that crystallization can either occur simultaneously with bilayer formation, as seems to be true for light-harvesting complex, or it can occur as a distinct step after detergent removal has been completed, e.g., porin forms large disordered sheets directly after detergent removal, which slowly become ordered (Jap et al., 1992). Because our methods grew out of functional studies of ion transport by Ca^{2+}-ATPase, we initially approached crystallization as a two-step process, first involving vesicle formation and purification, followed thereafter by vanadate-induced crystallization. As a result, our characterization of small proteoliposomes after reconstitution represents a novel approach to membrane protein crystallization.

Previous reconstitution studies with Ca^{2+}-ATPase at high lipid-to-protein ratios found special properties of $C_{12}E_8$ in producing two populations of vesicles, whereas Triton X-100 and octylglucoside produced vesicles with much more homogeneous distributions of protein (Levy et al., 1992). Our results with $C_{12}E_8$ at low lipid-to-protein ratios are completely consistent with these previous findings. We also found that virtually all Ca^{2+}-ATPase molecules were accessible to FITC and were therefore facing the outside of our reconstituted vesicles. Ultimately, this asymmetry leads to the ready formation of tubular crystals, which were shown in our three-dimensional reconstruction to comprise
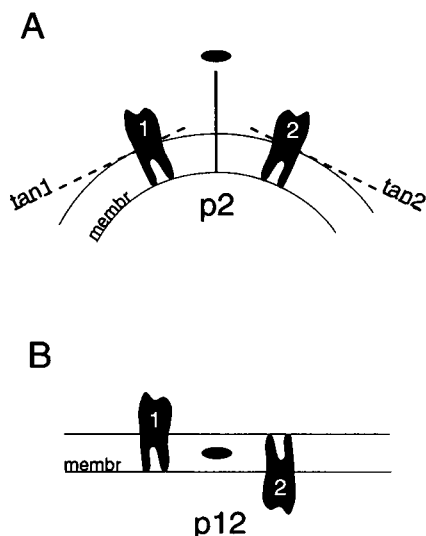
A

B
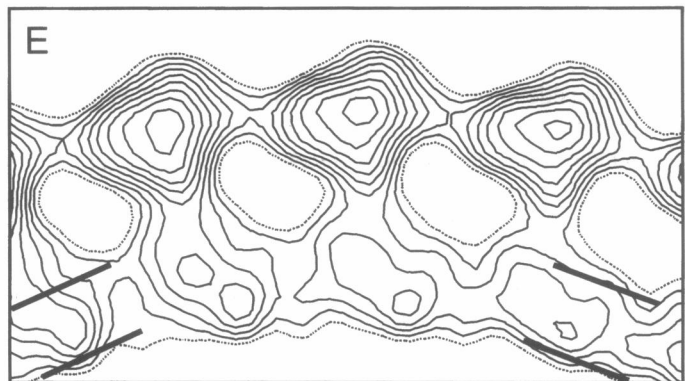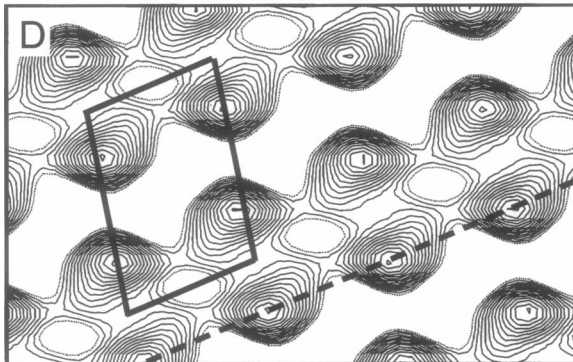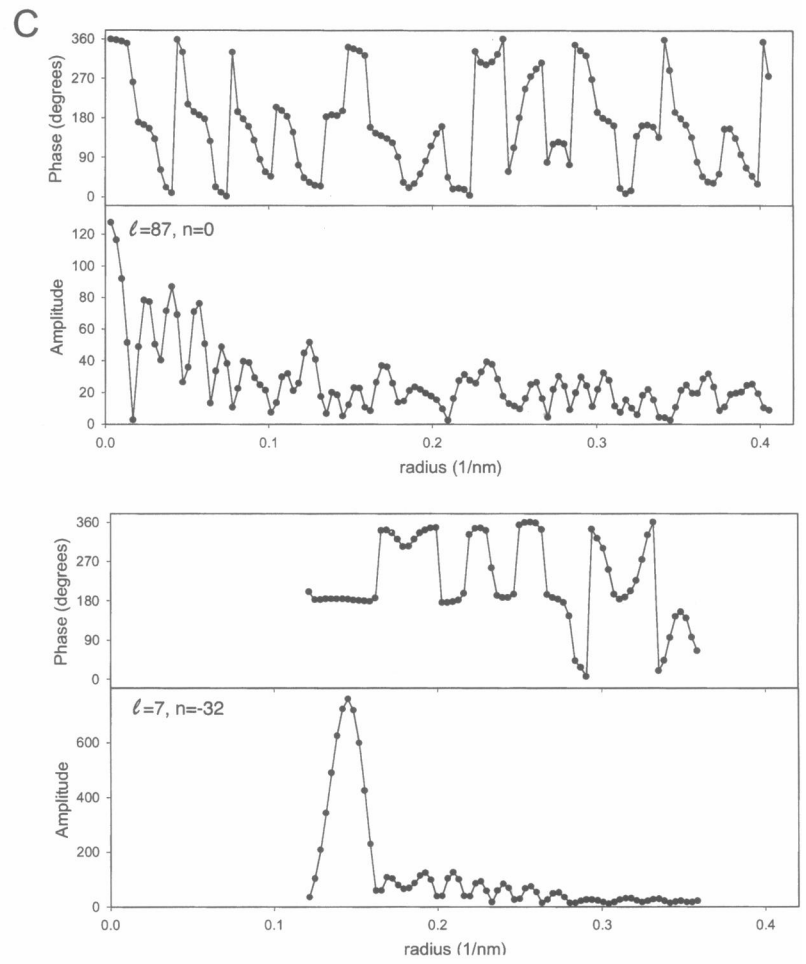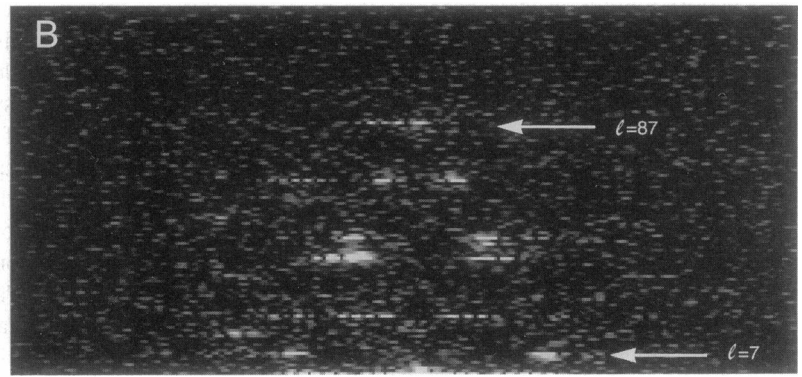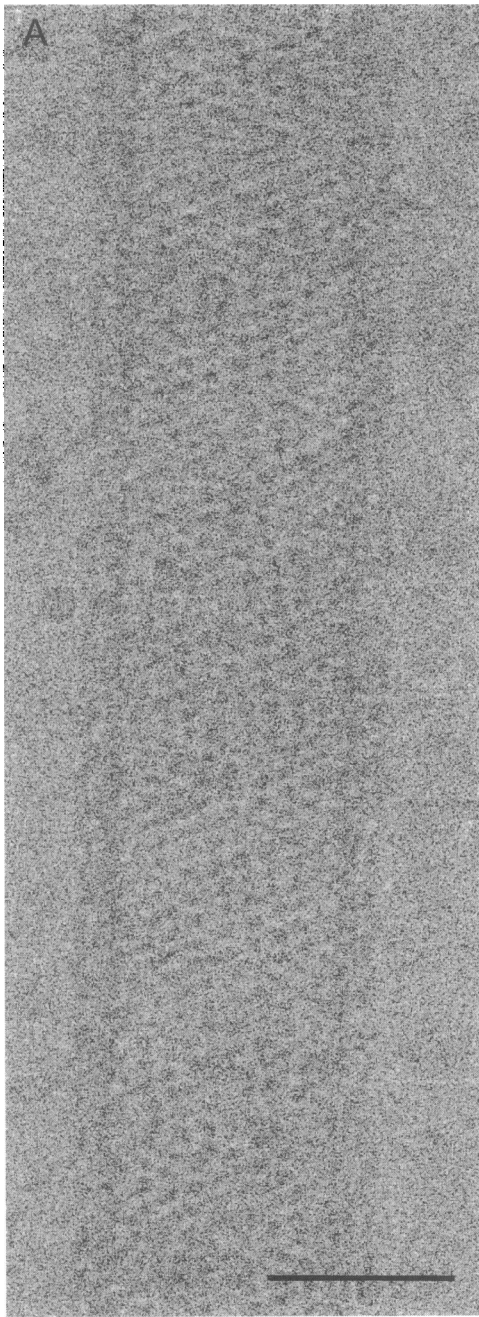
FIGURE 7 Symmetry and molecular packing in two-dimensional crystals. The membrane curvature in tubular crystals is compatible with a twofold symmetry axis perpendicular to the membrane (p2 in A), because inclined membrane tangents can still be related by such twofold symmetry. However, membrane curvature prevented by a twofold axis is in the plane of the membrane (p12 in B); in this case, the membrane tangents must be coplanar, thus favoring a planar crystal morphology.

unidirectionally oriented molecules with their bulky cytoplasmic domains on the outside of the vesicles (Fig. 6 E). Given that no crystallization forces were at work during our reconstitution, one might expect a random orientation of molecules and thus an accessibility of FITC to only half the molecules. However, the observed asymmetry may be explained in terms of the mechanism for Ca^{2+}-ATPase reconstitution proposed by Rigaud and colleagues (Levy et al., 1992; Rigaud et al., 1995), even though they did not explicitly address protein orientation. According to their mechanism, detergent solubilization results in a solution containing binary (lipid/detergent) and ternary (lipid/detergent/protein) micelles. If detergent is removed very rapidly, the binary and ternary micelles will be forced to coalesce with one another, leading to a homogeneous population of vesicles, all having the average lipid-to-protein ratio. If the detergent is removed slowly, it will be preferentially removed from ternary micelles, leading to their coalescence into protein-rich complexes. Thus partial detergent removal will result in a solution of detergent-saturated protein/lipid complexes together with binary micelles. In the cases of Triton X-100 and octylglucoside, the detergent mediates exchange of Ca^{2+}-ATPase between these two species, thus

maintaining the homogeneity of the system. However, $C_{12}E_8$ has been shown to be particularly inefficient in this exchange (Levy et al., 1992), so further slow detergent removal will produce a heterogeneous population of pure liposomes and protein-rich proteoliposomes, which is in fact what we observed. The inefficiency in this exchange appears to be related in part to the self-association of Ca^{2+}-ATPase, which is incompletely disrupted by solubilization with $C_{12}E_8$ (Levy et al., 1992; Rigaud et al., 1995). It seems reasonable to assume an orientational specificity in this self-association of Ca^{2+}-ATPase, in which case the proteins would likely adopt a preferred orientation during coalescence of ternary micelles, thus explaining the asymmetry of the resulting vesicles. Differences between $C_{12}E_8$ and Triton X-100 result from their differing interactions both with lipids and with Ca^{2+}-ATPase, which have previously been investigated in detail by Rigaud and colleagues (Levy et al., 1992; Rigaud et al., 1995).

This mechanism is also consistent with our results after slow removal of $C_{12}E_8$ from micellar mixtures at different lipid-to-protein ratios. According to the mechanism, the lipid-to-protein ratio in ternary micelles is governed by innate properties of Ca^{2+}-ATPase and perhaps by its tendency to self-associate. Any additional lipid will therefore exist in a separate population of binary micelles, and increasing the amount of lipid will simply increase the proportion of binary micelles. Because these ternary micelles give rise directly to proteoliposomes and binary micelles to liposomes, increasing the amount of lipid should simply increase the proportion of liposomes without affecting the population of proteoliposomes, and, indeed, this is what we observed. After sucrose density gradient purification, we determined the lipid-to-protein ratio in these proteoliposomes to be 1:2, which is consistent with the observed absence of liposomes when initial lipid-to-protein ratios were lower than 1:2. Interestingly, this is roughly the same ratio found in longitudinal SR, suggesting that this biological membrane is in fact maximally packed with Ca^{2+}-ATPase molecules.

We chose to use BioBeads SM2 for removal of detergent (Holloway, 1973), but microdialysis (Kühlbrandt, 1992) should in principle be equally effective. Although dialysis has been more popular for crystallization, polystyrene beads (a generic form of BioBeads) were used in the early crystallization of cytochrome reductase (Wingfield et al., 1979) and light-harvesting complex (Li and Hollingshead, 1982). The main reason we choose BioBeads was the very slow rate of dialysis for detergents with low critical micelle

FIGURE 6 Helical reconstruction of a frozen-hydrated, reconstituted tube. (A) Image of a frozen-hydrated tube (scale bar = 500 Å). (B) Top half of the computed Fourier transform from this tube; the layer line designated ℓ = 87 corresponds to ~26 Å resolution. (C) Amplitudes and phases along the two layer lines indicated in the transform (arrows in B); ℓ corresponds to the height and n to the Bessel order of each layer line. The twofold symmetry is evident from the phases, which closely correspond to either 0° or 180°. (D) A cylindrical section from the three-dimensional map cut parallel to the membrane surface through the cytoplasmic domain shows molecules arranged in antiparallel dimer ribbons; the parallelogram depicts the unit cell, which has dimensions a = 62.5 Å, b = 114.6 Å, and γ = 73°. (E) A section cut perpendicular to the membrane along the dimer ribbon (dotted line in D) shows that molecules all face the outside of the tube; the membrane surfaces are indicated by the parallel lines at either side in E.

concentrations (cmc for $C_{12}E_8$ ~0.08 mM or 0.04 mg/ml; Garavito et al., 1986), which thus required at least a week to complete the reconstitution. Detergent removal by BioBeads is generally much faster (minutes to hours) and can be controlled by adding small numbers of beads at strategic time intervals and/or by lowering the temperature (Levy et al., 1990a). Given the hydrophobic nature of these beads, adsorption of lipids or protein represents a potential problem. However, the relatively small pore size of beads should restrict adsorption of micellar material to the surface, whereas free detergent molecules diffuse inside the beads, and in fact the adsorption of lipid has been shown to be two orders of magnitude lower for lipid than for detergent (Levy et al., 1990a). Furthermore, no protein loss was observed, either during our reconstitutions of Ca^{2+}-ATPase or during crystallization studies with a variety of other membrane proteins (Levy et al., 1990a; Rigaud et al., 1997).

Formation of tubes from vesicles

Although two-dimensional arrays readily formed in proteo-liposomes obtained directly after detergent removal, tubes did not grow at this early stage (Fig. 2). This is similar to results usually obtained with SR, which generally produce crystalline vesicles and occasional short tubes (Fig. 1 A). In rare preparations (Fig. 1 B), large SR vesicles are obtained and, in this case, long tubes can be obtained. This suggests that crystal contacts provide the driving force behind tube formation, but that vesicles are not generally able to fuse to allow extended growth of the crystal lattice. However, cycles of freeze-thaw after reconstitution produced vesicle aggregates from which tubes did grow, provided that the appropriate lipids were added during crystallization (Fig. 5). Unlike classical results with pure liposomes, freeze-thaw did not significantly increase the size of vesicles by fusion, but primarily produced these aggregates. Although we have no evidence for a specific mechanism, we imagine that this aggregation is due both to protein-protein interactions and to defects within the bilayers, which result in exposed hydrophobic surfaces during freeze-thaw. The resulting aggregates are inherently unstable and thus provide a reservoir of protein and lipid, which can be recruited during crystallization and which therefore lead to growth of long tubes. Given the nonbilayer phases adopted by high concentrations of PE, PA, and PS (Cornelius, 1991; Gruner, 1985), we hypothesize that their promotion of tube formation (see Table 1) is due to an increased recruitability of material from the aggregates, which is a result of an increase in bilayer defects. We also found that addition of $C_{12}E_8$ after freeze-thaw also produced tubes, even in the absence of either PE or PA, and this suggests that subsolubilizing amounts of $C_{12}E_8$ also create bilayer defects. The inhibitory influence of cholesterol on tube formation could be due either to an effect on recruitment, or to a negative effect on crystal packing in the tubes, e.g., by opposing curvature of the bilayer.

Application to other proteins

Although our reconstitution methods have been optimized for Ca^{2+}-ATPase, the principles are relevant to a wide variety of other membrane proteins. In particular, the family of P-type ion pumps have a similar molecular architecture, and crystals of both Na^+/K^+-ATPase (Hebert et al., 1985; Mohraz et al., 1987) and H^+/K^+-ATPase (Rabon et al., 1986) have been induced in native membranes by the addition of vanadate. Like tubes of Ca^{2+}-ATPase, these other crystals have p2 symmetry with molecules arranged into dimer ribbons, but so far these crystals have been poorly ordered, suggesting reconstitution studies as a plausible avenue for future structural studies. Crystals of plasma membrane Ca^{2+}-ATPase have not been reported (but see Pikula et al., 1991) and would certainly require reconstitution given their low density in the plasma membrane. The same is true of the vast majority of other P-type ion pumps, which represent a large family with a diverse catalog of functions. Another potential use of reconstitution is to form cocrystals with some effector molecule. In particular, cardiac Ca^{2+}-ATPase is regulated by a small membrane protein, phospholamban, for which little structural information exists (Tada and Kadoma, 1989). We have previously characterized the coreconstitution of these two proteins and verified their functional association at high lipid-to-protein ratios (Reddy et al., 1995, 1996). Recently we have decreased this ratio and have been successful in obtaining tubular crystals from preparations containing both Ca^{2+}-ATPase and phospholamban at physiologically reasonable stoichiometries, and we are hoping to use these tubes for the structural investigation of phospholamban and its association with Ca^{2+}-ATPase.

REFERENCES

Aebi, U., W. E. Fowler, E. L. Buhle, and P. R. Smith. 1984. Electron microscopy and image processing applied to the study of protein structure and protein-protein interactions. *J. Ultrastruct. Res.* 88:143–176.

Akiba, T., C. Toyoshima, T. Matsunaga, M. Kawamoto, T. Kubota, K. Fukuyama, K. Namba, and H. Matsubara. 1996. Three-dimensional structure of bovine cytochrome bc_1 complex by electron cryomicroscopy and helical image reconstruction. *Nature Struct. Biol.* 3:553–561.

Amos, L. A., R. Henderson, and P. N. T. Unwin. 1982. Three-dimensional structure determination by electron microscopy of two-dimensional crystals. *Prog. Biophys. Mol. Biol.* 39:183–231.

Blaurock, A. E., and W. Stoeckenius. 1971. Structure of the purple membrane. *Nature New Biol.* 233:152–155.

Brisson, A., and P. N. T. Unwin. 1984. Tubular crystals of acetylcholine receptor. *J. Cell. Biol.* 99:1202–1211.

Castellani, L., P. M. Hardwicke, and P. Vibert. 1985. Dimer ribbons in the three-dimensional structure of sarcoplasmic reticulum. *J. Mol. Biol.* 185:579–594.

Champeil, P., S. Buschlen-Boucly, F. Bastide, and C. Gary-Bobo. 1978. Sarcoplasmic reticulum ATPase: spin labeling detection of ligand-induced changes in the relative reactivities of certain sulfhydryl groups. *J. Biol. Chem.* 253:1179–1186.

Chen, P. S., T. Y. Toribara, and H. Warner. 1956. Microdetermination of phosphorous. *Anal. Chem.* 28:1756–1758.

Chester, D. W., L. G. Herbette, R. P. Mason, A. F. Joslyn, and D. J. Triggle. 1987. Diffusion of dihydropyridine calcium channel antagonists in cardiac sarcolemmal lipid multibilayers. *Biophys. J.* 52:1021–1030.

Cornelius, F. 1991. Functional reconstitution of the sodium pump: kinetics of exchange reactions performed by reconstituted Na/K-ATPase. *Biochim. Biophys. Acta.* 1071:19–66.

Deisenhofer, J., O. Epp, K. Miki, R. Huber, and H. Michel. 1985. Structure of the protein subunits in the photosynthetic reaction centre of *Rhodopseudomonas viridis* at 3 Å resolution. *Nature.* 318:618–624.

DeRosier, D. J., and P. B. Moore. 1970. Reconstruction of three-dimensional images from electron micrographs of structures with helical symmetry. *J. Mol. Biol.* 52:355–369.

Dolder, M., A. Engel, and M. Zulauf. 1996. The micelle to vesicle transition of lipids and detergents in the presence of a membrane protein: towards a rationale for 2D crystallization. *FEBS Lett.* 382:203–208.

Dux, L., and A. Martonosi. 1983. Two-dimensional arrays of proteins in sarcoplasmic reticulum and purified Ca²⁺-ATPase vesicles treated with vanadate. *J. Biol. Chem.* 258:2599–2603.

Dux, L., K. A. Taylor, H. P. Ting-Beall, and A. Martonosi. 1985. Crystallization of the Ca²⁺-ATPase of sarcoplasmic reticulum by calcium and lanthanide ions. *J. Biol. Chem.* 260:11730–11743.

Eletr, S., and G. Inesi. 1972. Phospholipid orientation in sarcoplasmic reticulum membranes: spin-label ESR and proton NMR studies. *Biochim. Biophys. Acta.* 282:174–179.

Engel, A., A. Hoenger, A. Hefti, C. Henn, R. C. Ford, J. Kistler, and M. Zulauf. 1992. Assembly of 2-D membrane protein crystals: dynamics, crystal order, and fidelity of structure analysis by electron microscopy. *J. Struct. Biol.* 109:219–234.

Garavito, R. M., Z. Markovic-Housley, and J. Jenkins. 1986. The growth and characterization of membrane protein crystals. *J. Crystal Growth.* 76:701–709.

Garavito, R. M., D. Picot, and P. J. Loll. 1996. Strategies for crystallizing membrane proteins. *J. Bioenerg. Biomembr.* 28:13–27.

Gruner, S. 1985. Intrinsic curvature hypothesis for biomembrane lipid composition: a role for nonbilayer lipids. *Proc. Natl. Acad. Sci. USA.* 82:3665–3669.

Hebert, H., E. Skriver, and A. B. Maunsbach. 1985. Three-dimensional structure of renal Na, K-ATPase determined by electron microscopy of membrane crystals. *FEBS Lett.* 187:182–186.

Henderson, R., J. M. Baldwin, T. A. Ceska, F. Zemlin, E. Beckmann, and K. H. Downing. 1990. Model for the structure of bacteriorhodopsin based on high-resolution electron cryo-microscopy. *J. Mol. Biol.* 213:899–929.

Henderson, R., and P. N. T. Unwin. 1975. Three-dimensional model of purple membrane obtained from electron microscopy. *Nature.* 257:28–32.

Holloway, P. W. 1973. A simple procedure for removal of Triton X-100 from protein samples. *Anal. Biochem.* 53:304–307.

Iwata, S., C. Ostermeier, B. Ludwig, and H. Michel. 1995. Structure at 2.8 Å resolution of cytochrome c oxidase from *Paracoccus denitrificans. Nature.* 376:660–669.

Jap, B. K., M. Zulauf, T. Scheybani, A. Hefti, W. Baumeister, U. Aebi, and A. Engel. 1992. 2D crystallization: from art to science. *Ultramicroscopy.* 46:45–84.

Karon, B. S., E. Mahaney, and D. D. Thomas. 1994. Halothane and cyclopiazonic acid modulate Ca-ATPase oligomeric state and function in sarcoplasmic reticulum. *Biochemistry.* 33:13928–13937.

Kühlbrandt, W. 1988. Three-dimensional crystallization of membrane proteins. *Q. Rev. Biophys.* 21:429–477.

Kühlbrandt, W. 1992. Two-dimensional crystallization of membrane proteins. *Q. Rev. Biophys.* 25:1–49.

Kühlbrandt, W., and D. N. Wang. 1991. Three-dimensional structure of plant light-harvesting complex determined by electron crystallography. *Nature.* 350:130–134.

Levy, D., A. Bluzat, M. Seigneuret, and J.-L. Rigaud. 1990a. A systematic study of liposome and proteoliposome reconstitution involving Bio-Bead-mediated Triton X-100 removal. *Biochim. Biophys. Acta.* 1025:179–190.

Levy, D., A. Gulik, A. Bluzat, and J.-L. Rigaud. 1992. Reconstitution of the sarcoplasmic reticulum Ca⁺⁺-ATPase: mechanisms of membrane protein insertion into liposomes during reconstitution procedures involving detergents. *Biochim. Biophys. Acta.* 1107:283–298.

Levy, D., A. Gulik, M. Seigneuret, and J.-L. Rigaud. 1990b. Phospholipid vesicle solubilization and reconstitution by detergents. Symmetrical analysis of the two processes using octaethylene glycol mono-n-dodecyl ether. *Biochemistry.* 29:9480–9488.

Levy, D., M. Seigneuret, A. Bluzat, and J.-L. Rigaud. 1990c. Evidence for proton countertransport by the sarcoplasmic reticulum Ca²⁺-ATPase during calcium transport in reconstituted proteoliposomes with low ionic permeability. *J. Biol. Chem.* 265:19524–19534.

Li, J., and C. Hollingshead. 1982. Formation of crystalline arrays of chlorophyll a/b-light-harvesting protein by membrane reconstitution. *Biophys. J.* 37:363–370.

Lowry, O. H., N. J. Rosebrough, A. L. Farr, and R. J. Randall. 1951. Protein measurement with the Folin phenol reagent. *J. Biol. Chem.* 193:265–275.

MacLennan, D. H. 1970. Purification and properties of an adenosine triphosphatase from sarcoplasmic reticulum. *J. Biol. Chem.* 245:4508–4518.

Mannella, C. A. 1984. Phospholipase-induced crystallization of channels in mitochondrial outer membranes. *Science.* 224:165–166.

Markwell, M. H., S. M. Hass, L. L. Beiber, and N. E. Tolbert. 1978. A modification of the Lowry procedure to simplify protein determination in membrane and lipoprotein samples. *Anal. Biochem.* 87:206–210.

Meissner, G., G. E. Conner, and S. Fleischer. 1973. Isolation of sarcoplasmic reticulum by zonal centrifugation and purification of Ca²⁺-pump and Ca²⁺-binding proteins. *Biochim. Biophys. Acta.* 298:246–269.

Mitchinson, C., A. F. Wilderspin, B. J. Trinnaman, and N. M. Green. 1982. Identification of a labelled peptide after stoichiometric reaction of fluorescein isothiocyanate with the Ca²⁺-dependent adenosine triphosphatase of sarcoplasmic reticulum. *FEBS Lett.* 146:87–92.

Mohraz, M., M. V. Simpson, and P. R. Smith. 1987. The three-dimensional structure of the Na,K-ATPase from electron microscopy. *J. Cell. Biol.* 105:1–8.

Pederson, P. L., and E. Carafoli. 1987. Ion motive ATPases. 1. Ubiquity, properties, and significance to cell function. *Trends Biol. Sci.* 12:146–150.

Picot, D., P. J. Loll, and R. M. Garavito. 1994. The x-ray crystal structure of the membrane protein prostaglandin H₂ synthase-1. *Nature.* 367:243–249.

Pikula, S., A. Wrzosek, and K. S. Famulski. 1991. Long-term stabilization and crystallization of (Ca²⁺Mg²⁺)-ATPase of detergent solubilized erythrocyte plasma membrane. *Biochim. Biophys. Acta.* 1061:206–214.

Rabon, E., M. Wilke, G. Sachs, and G. Zampighi. 1986. Crystallization of the gastric H,K-ATPase. *J. Biol. Chem.* 261:1434–1439.

Reddy, L. G., L. R. Jones, S. E. Cala, J. J. O'Brian, S. A. Tatulian, and D. L. Stokes. 1995. Functional reconstitution of recombinant phospholamban with rabbit skeletal Ca-ATPase. *J. Biol. Chem.* 270:9390–9397.

Reddy, L. G., L. R. Jones, R. C. Pace, and D. L. Stokes. 1996. Purified, reconstituted cardiac Ca²⁺-ATPase is regulated by phospholamban but not by direct phosphorylation with Ca²⁺/calmodulin-dependent protein kinase. *J. Biol. Chem.* 271:14964–14970.

Revel, J. P., and J. J. Karnovsky. 1967. Hexagonal array of subunits in intercellular junctions of the mouse heart and liver. *J. Cell. Biol.* 33:C7–C12.

Rigaud, J.-L., G. Mosser, J.-J. Lacapere, A. Olofsson, D. Levy, J.-L. Ranck. 1997. Bio-beads: an efficient strategy for two dimensional crystallization of membrane proteins. *J. Struct. Biol.* 118:226–235.

Rigaud, J.-L., B. Pitard, and D. Levy. 1995. Reconstitution of membrane proteins into liposomes: application to energy-transducing membrane proteins. *Biochim. Biophys. Acta.* 1231:223–246.

Sagara, Y., J. B. Wade, and G. Inesi. 1992. A conformational mechanism for formation of a dead-end complex by the sarcoplasmic reticulum ATPase with thapsigargin. *J. Biol. Chem.* 267:1286–1292.

Skriver, E., A. B. Maunsbach, and P. L. Jorgensen. 1981. Formation of two-dimensional crystals in pure membrane-bound Na^+/K^+-ATPase. *FEBS Lett.* 131:219–222.

Stokes, D. L., and N. M. Green. 1990. Three-dimensional crystals of Ca-ATPase from sarcoplasmic reticulum: symmetry and molecular packing. *Biophys. J.* 57:1–14.

Tada, M., and M. Kadoma. 1989. Regulation of the Ca^{2+} pump ATPase by cAMP-dependent phosphorylation of phospholamban. *Bioessays.* 10: 157–163.

Taylor, K., L. Dux, and A. Martonosi. 1984. Structure of the vanadate-induced crystals of sarcoplasmic reticulum Ca^{2+}-ATPase. *J. Mol. Biol.* 174:193–204.

Taylor, K. A., L. Dux, and A. Martonosi. 1986a. Three-dimensional reconstruction of negatively stained crystals of the Ca^{++}-ATPase from muscle sarcoplasmic reticulum. *J. Mol. Biol.* 187:417–427.

Taylor, K. A., M. H. Ho, and A. Martonosi. 1986b. Image analysis of the Ca^{2+}-ATPase from sarcoplasmic reticulum. *Ann. N.Y. Acad. Sci.* 483: 31–43.

Toyoshima, C., H. Sasabe, and D. L. Stokes. 1993a. Three-dimensional cryo-electron microscopy of the calcium ion pump in the sarcoplasmic reticulum membrane. *Nature.* 362:469–471.

Toyoshima, C., and N. Unwin. 1988. Contrast transfer for frozen-hydrated specimens: determination from pairs of defocused images. *Ultramicroscopy.* 25:279–292.

Toyoshima, C., and N. Unwin. 1990. Three-dimensional structure of the acetylcholine receptor by cryoelectron microscopy and helical image reconstruction. *J. Cell. Biol.* 111:2623–2635.

Toyoshima, C., K. Yonekura, and H. Sasabe. 1993b. Contrast transfer for frozen-hydrated specimens. II. Amplitude contrast at very low frequencies. *Ultramicroscopy.* 48:165–176.

Wang, D. N., W. Kühlbrandt, V. E. Sarabia, and R. A. F. Reithmeier. 1993. Two-dimensional structure of the membrane domain of human band 3, the anion transport protein of the erythrocyte membrane. *EMBO J.* 12:2233–2239.

Warne, A., D. N. Wang, and M. Saraste. 1995. Purification and two-dimensional crystallization of bacterial cytochrome oxidases. *Eur. J. Biochem.* 234:443–451.

Warren, G. B., P. A. Toon, N. J. M. Birdsall, A. G. Lee, and J. C. Metcalfe. 1974. Reconstitution of a calcium pump using defined membrane components. *Proc. Natl. Acad. Sci. USA.* 71:622–626.

Weiss, M. S., T. Wacker, J. Weckesser, W. Welte, and G. E. Schulz. 1990. The three-dimensional structure of porin from *Rhodobacter capsulatus* at 3 Å resolution. *FEBS Lett.* 267:268–272.

Wingfield, P., T. Arad, K. Leonard, and H. Weiss. 1979. Membrane crystals of ubiquinone: cytochrome c reductase from *Neurospora mitochondria. Nature.* 280:696–697.

Yonekura, K., D. L. Stokes, H. Sasabe, C. Toyoshima. 1997. The ATP-binding site of Ca^{2+}-ATPase revealed by electron image analysis. *Biophys. J.* 72:997–1005.

Yu, X., S. Carroll, J.-L. Rigaud, and G. Inesi. 1993. H^+ countertransport and electrogenecity of the sarcoplasmic reticulum Ca^{2+} pump in reconstituted proteoliposomes. *Biophys. J.* 64:1232–1242.